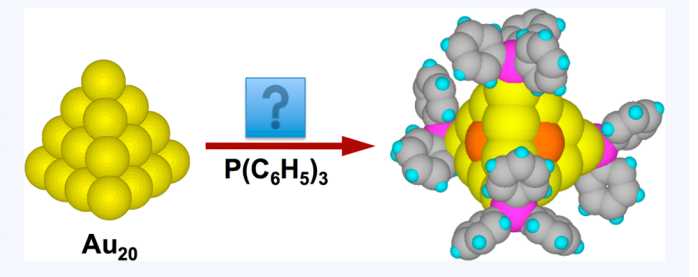


Toward Solution Syntheses of the Tetrahedral Au₂₀ Pyramid and **Atomically Precise Gold Nanoclusters with Uncoordinated Sites**

Published as part of the Accounts of Chemical Research special issue "Toward Atomic Precision in Nanoscience". Qian-Fan Zhang, [†] Xuenian Chen, [‡] and Lai-Sheng Wang*, [†]

CONSPECTUS: A long-standing objective of cluster science is to discover highly stable clusters and to use them as models for catalysts and building blocks for cluster-assembled materials. The discovery of catalytic properties of gold nanoparticles (AuNPs) has stimulated wide interests in gaseous size-selected gold clusters. Ligand-protected AuNPs have also been extensively investigated to probe their sizedependent catalytic and optical properties. However, the need to remove ligands can introduce uncertainties in both the structures and sizes of ligand-protected AuNPs for catalytic



applications. Ideal model catalysts should be atomically precise AuNPs with well-defined structures and uncoordinated surface sites as in situ active centers. The tetrahedral (T_d) Au₂₀ pyramidal cluster, discovered to be highly stable in the gas phase, provided a unique opportunity for such an ideal model system. The T_d -Au₂₀ consists of four Au(111) faces with all its atoms on the surface. Bulk synthesis of T_d -Au₂₀ with appropriate ligands would allow its catalytic and optical properties to be investigated and harnessed. The different types of its surface atoms would allow site-specific chemistry to be exploited. It was hypothesized that if the four corner atoms of T_d -Au₂₀ were coordinated by ligands the cluster would still contain 16 uncoordinated surface sites as potential in situ catalytically active centers.

Phosphine ligands were deemed to be suitable for the synthesis of T_d -Au₂₀ to maintain the integrity of its pyramidal structure. Triphenyl-phosphine-protected T_d -Au₂₀ was first observed in solution, and its stability was confirmed both experimentally and theoretically. To enhance the synthetic yield, bidentate diphosphine ligands [(Ph)₂P(CH₂)_nP(Ph)₂ or Lⁿ] with different chain lengths were explored. It was hypothesized that diphosphine ligands with the right chain length might preferentially coordinate to the T_d-Au₂₀. Promising evidence was initially obtained by the formation of the undecagold by the L³ ligand. When the L⁸ diphosphine ligand was used, a remarkable Au₂₂ nanocluster with eight uncoordinated Au sites, Au₂₂(L⁸)₆₁, was synthesized. With a tetraphosphine-ligand (PP₃), a new Au₂₀ nanocluster, $[Au_{20}(PP_3)_4]Cl_4$, was isolated with high yield. The crystal structure of the new Au₂₀ core did not reveal the expected pyramid but rather an intrinsically chiral gold core. The surface of the new chiral-Au₂₀ was fully coordinated, and it was found to be highly stable chemically.

The Au₂₂(L⁸)₆ nanocluster represents the first and only gold core with uncoordinated gold atoms, providing potentially eight in situ catalytically active sites. The Au₂₂ nanoclusters dispersed on oxide supports were found to catalyze CO oxidation and activate H2 without ligand removal. With further understanding about the formation mechanisms of gold nanoclusters in solution, it is conceivable that T_{d} -Au₂₀ can be eventually synthesized, allowing its novel catalytic and optical properties to be explored. More excitingly, it is possible that a whole family of new atomically precise gold nanoclusters can be created with different phosphine ligands.

1. INTRODUCTION

Gold is known to be the most stable metal and has been used in coinage or jewelry for millennia. However, when gold is reduced to sizes less than 100 nm, the chemical and physical properties of the resulting Au nanoparticles (AuNPs) can change significantly, due to the appearance of quantum effects and the large ratio of low-coordinated surface atoms. The development of solution synthesis and surface modification methods for AuNPs has led to extensive investigations of their size-dependent properties and potential applications in diverse

fields.^{1,2} However, the compositions and structures of such AuNPs are usually not defined precisely at the atomic level for two main reasons: (a) the solution synthesis and purification methods cannot reach 100% monodispersity for the metal core; (b) electron microscopy, used to characterize the size and shape of AuNPs, cannot resolve light atoms in the coordination sphere. The poorly defined compositions and

Received: June 2, 2018 Published: August 2, 2018



Department of Chemistry, Brown University, Providence, Rhode Island 02912, United States

^{*}School of Chemistry and Chemical Engineering, Henan Key Laboratory of Boron Chemistry and Advanced Energy Materials, Henan Normal University, Xinxiang, Henan 453007, China

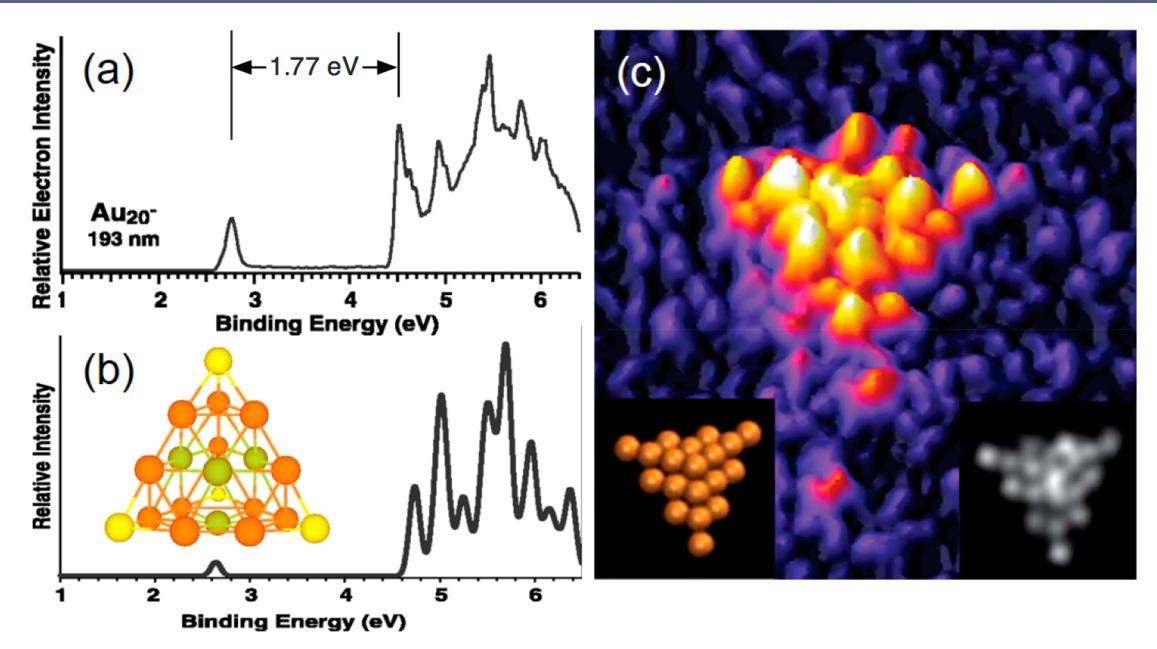


Figure 1. (a) Experimental photoelectron spectrum of the $\mathrm{Au_{20}}^-$ anion. The energy gap of 1.77 eV is labeled. (b) The tetrahedral structure of the $\mathrm{Au_{20}}^-$ cluster (insert) and its simulated photoelectron spectrum. (c) HAADF-STEM image (2.8 × 2.8 nm²) of a $\mathrm{Au_{20}}$ cluster (left inset shows the orientation of the $\mathrm{Au_{20}}$ cluster; the right inset is the simulated STEM image). Panels a and b reproduced with permission from ref 9. Copyright 2003 American Association for the Advancement of Science. Panel c reproduced with permission from ref 23. Copyright 2012 The Royal Society of Chemistry.

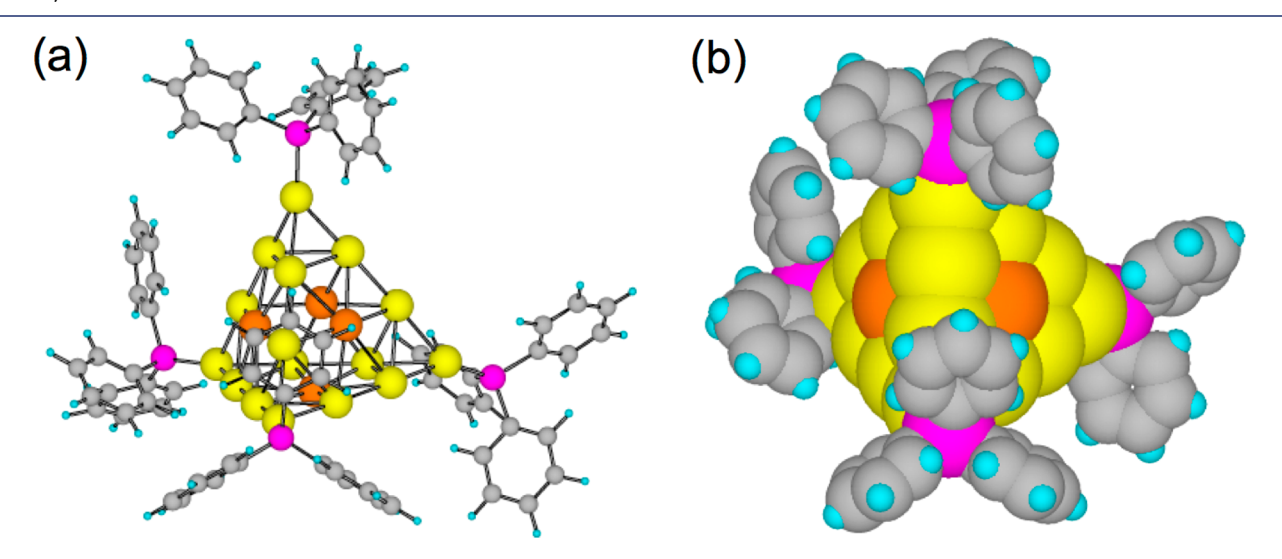


Figure 2. (a) Computed structure of $Au_{20}(PPh_3)_4$ and (b) The van der Waals surface of $Au_{20}(PPh_3)_4$. Reproduced with permission from ref 36. Copyright 2004 American Chemical Society.

structures could raise serious problems of reliability and reproducibility for studies of such AuNPs. Therefore, solution syntheses of well-defined atomically precise AuNPs or Au nanoclusters (AuNCs) are highly desirable.

The predicament of the synthesis of AuNCs in solution is readily resolved by gaseous Au clusters. In the gas phase, every cluster is atomically precise by definition, because the cluster sizes can be determined and selected by mass spectrometry and the cluster structures can be obtained through experimental and theoretical investigations. The structures of size-selected gaseous Au clusters containing several dozens of atoms ($\sim 0.3-1.5$ nm) have been characterized thus far. These clusters are ideal model systems to investigate the catalytic properties of AuNPs, a especially for elucidating the intrinsic properties of the Au core.

Among all the gas-phase Au clusters, Au_{20} was the most remarkable. Its large HOMO–LUMO gap (1.77 eV) as revealed by photoelectron spectroscopy of the negatively charged Au_{20}^- (Figure 1a) suggested that neutral Au_{20} upon electron detachment should be highly stable. Its tetrahedral (T_d) structure (Figure 1b) has the same atomic arrangement as the face-centered cubic bulk gold. Yet, its 1.77 eV energy gap indicates a semiconductor, and it should have a blue color. Most interestingly, the Au_{20} pyramid consists of four $\mathrm{Au}(111)$ faces with all 20 atoms on its surface. Its structure has been confirmed by infrared spectroscopy, trapped-ion electron diffraction, infrared spectroscopy, trapped-ion electron diffraction, and high-angle annular dark-field scanning transmission electron microscopy (HAADF-STEM) (Figure 1c). Many interesting properties have been revealed for the T_d - Au_{20} over the past decade: (a) larger Au clusters are found

to contain the T_d -Au₂₀ fragment; 18,20 (b) it is highly active catalytically; $^{24-31}$ (c) it has unique optical properties. $^{32-35}$

However, the bare Au₂₀ pyramid can only be produced in small quantities in molecular beams in the gas phase. In order to study and harness the potentially interesting properties of the golden pyramid, an effective synthetic method has to be developed to produce bulk quantities with ligand protection to prevent cluster-cluster aggregation. This Account focuses on our efforts to achieve solution synthesis of the T_d -Au₂₀ using phosphine-based ligands.³⁶ During the journey toward this ultimate goal, several interesting phosphine-protected AuNCs have been discovered.^{37–40} In particular, we have synthesized with a diphosphine ligand a Au₂₂ cluster that contains eight uncoordinated Au sites.³⁸ This cluster represents the first AuNC with in situ catalytically active centers, which have been shown to catalyze CO oxidation and hydrogen evolution. 41-43 Atomically precise AuNCs with thiolate ligands⁴⁴ are covered by other Accounts in this special issue and will not be discussed here.

2. OBSERVATION OF PHOSPHINE-PROTECTED Au₂₀ PYRAMID IN SOLUTION

Because of potential cluster-cluster aggregation, the Au₂₀ pyramid must be protected by ligands if bulk samples are to be obtained. To maintain the unique structural and electronic properties of the T_d -Au₂₀, the ligands have to be carefully chosen. Thiolate ligands have strong chemical interactions with Au and would alter the electronic and geometrical structure of the T_d -Au₂₀. Thus, we considered initially the neutral PPh₃ ligands,³⁶ which form only dative bonds to Au and offer the possibility that both the T_d -Au₂₀ core and its unique electronic structure would not be altered. Because the four apex sites of T_d -Au₂₀ are more reactive, we reasoned that the bulky triphenyl phosphine (PPh₃) ligand might only coordinate to these sites, leaving 16 uncoordinated surface sites for chemisorption and catalysis. Theoretical calculations suggested that the Au₂₀(PPh₃)₄ complex indeed possesses high stability (Figure 2).³⁶ The only effect the phosphine ligands had on the Au₂₀ core was that the four face-center Au atoms (orange-colored in Figure 2) tended to be pushed outward from the four Au(111) faces: the calculated distance between the face-center atoms was increased from 3.1 Å in bare Au₂₀ to 3.4 Å in Au₂₀(PPh₃)₄. But the ligated complexes still maintained a large HOMO-LUMO gap: 1.44 eV in Au₂₀(PPh₃)₄³⁶ compared to 1.77 eV in the bare Au₂₀ pyramid.⁹

Phosphine-coordinated Au clusters with low nuclearities were well-known, such as the undecagold and the icosahedral $\mathrm{Au_{13}}^{.45-50}$ Our initial attempt to synthesize $\mathrm{Au_{20}}(\mathrm{PPh_3})_4$ utilized a two-phase system similar to that used for the synthesis of small phosphine-stabilized AuNPs.⁵¹ Basically, a solution of ClAuPPh3 dissolved in a toluene/water mixed solvent was reduced by NaBH4. In the ensuing nucleation, AuNPs with different sizes were produced. Using highresolution electrospray ionization mass spectrometry (ESI-MS), we detected a Au₂₀(PPh₃)₈²⁺ complex (Figure 3a), which was inferred to possess the expected tetrahedral Au₂₀ core with the four apex Au atoms and the four face-centered Au atoms coordinated by the PPh3 ligands. As can be seen from Figure 2b, there is still room to accommodate additional ligands in the face centered positions. It was shown that the four face centered ligands were more weakly bound and could be easily removed by collision-induced dissociation (Figure 3b). However, the synthesis was not selective, and the yield was

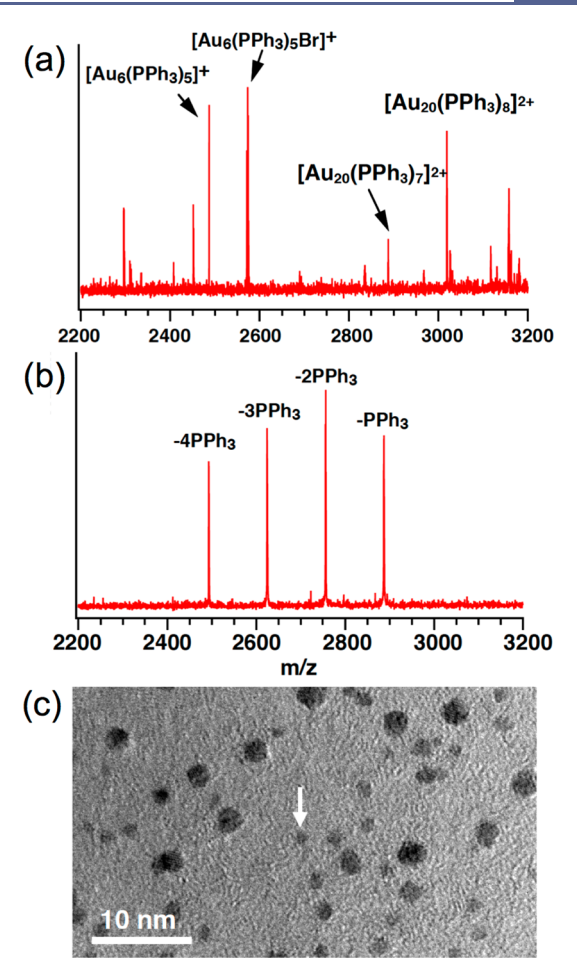


Figure 3. (a) ESI-MS of Au–PPh₃ complexes. (b) MS/MS of the $[\mathrm{Au}_{20}(\mathrm{PPh}_3)_8]^{2+}$ ion by collision-induced dissociation. (c) TEM image of Au–PPh₃ nanoparticles; the arrow points to a possible Au₂₀ cluster. Reproduced with permission from ref 36. Copyright 2004 American Chemical Society.

very low. Many large AuNPs in the size range of 1-4 nm were observed from high-resolution TEM (Figure 3c). Clearly, better synthetic strategies need to be devised to allow large quantities of the T_d -Au₂₀ samples to be obtained.

CONTROLLING THE SYNTHESIS OF AUNCS BY DIPHOSPHINE LIGANDS

To search for better synthetic methods for the T_d -Au₂₀, we took a new strategy by exploring different phosphine ligands and nucleation conditions while monitoring the reaction progress using ESI-MS.³⁷ We tested a series of α,ω bis(diphenylphosphino) alkanes of the general formula, $P(Ph)_2(CH_2)_nP(Ph)_2$ (n = 1-6) (abbreviated as Lⁿ), which were then available commercially. We hypothesized that the bidentate ligands might impose different stereoeffects to achieve size selectivity, depending on the chain length. In the synthesis, ClAuPPh3 dissolved in trichloromethane was reduced by borane-tert-butylamine in the presence of a selected L^{n} ligand. ESI-MS was used to monitor the cluster distributions during the experiment. Although we did not find the conditions to produce the desired T_d -Au₂₀, we did observe that the diphosphine ligands with n = 3-6 exhibited a high degree of size selectivity (Figure 4),³⁷ giving rise to a simple method to synthesize monodispersed Au_N clusters with $N \leq$ 11. In particular, high selectivity for undecagold was observed

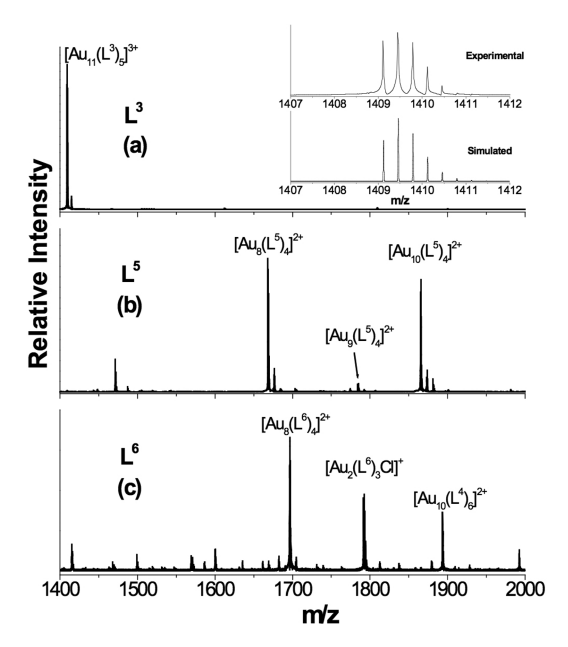


Figure 4. ESI-MS characterization of Au clusters stabilized with the indicated diphosphine ligand (L^n). The inset in panel a shows the isotopic pattern of the $\left[\mathrm{Au}_{11}(L^3)_5\right]^{3+}$ mass peak and the simulated isotopic pattern. Reproduced with permission from ref 37. Copyright 2006 American Chemical Society.

with the L³ ligand (Figure 4a). This work was subsequently confirmed, and the mechanisms of the cluster selectivity were further investigated. $^{52-54}$ We were limited then to n=1-6 because these were the only commercially available diphosphine ligands at the time.

CRYSTALLIZATION OF THE FIRST DIPHOSPHINE-PROTECTED GOLD NANOCLUSTERS WITH UNCOORDINATED SURFACE SITES: Au₂₂(L⁸)₆

With the promising observation of Au_N core size selectivity by different L^n diphosphine ligands, we synthesized a library of larger ligands with n = 7-12. Recognizing that the presence of free PPh₃ ligand could etch the Au_N cores during nucleation in solution, we prepared the Au precursors from ClAuPPh₃ to $Cl_2Au_2(L^n)$ by eliminating PPh₃, in order to obtain larger clusters. When we used NaBH₄ to reduce $Cl_2Au_2(L^8)$, we

indeed observed a AuNC with a large Au_N core, on the basis of UV-vis absorption. After purification and single-crystal growth, the formula and structure of the new AuNC were determined to be $Au_{22}(L^8)_{61}$, which consisted of two Au_{11} units bridged by four L⁸ ligands (Figure 5).³⁸ There was one L⁸ ligand coordinated to two Au atoms in each Au₁₁ unit. The dimension of the Au₂₂ core was 1.4 nm along its long axis (Figure 5c). The most unique structural feature of $Au_{22}(L^8)_6$ was the eight Au atoms at the interface of the two Au₁₁ units. These eight atoms were not coordinated, although they were protected to some degree by the aliphatic carbon chains via van der Waals interactions (Figure 5a). The Au-Au bonds at the interface were fairly short (2.64-2.65 Å). In comparison to the well-known undecagold $[Au_{11}]^{3+}$ core, 45,46 the Au_{11} units in Au₂₂(L⁸)₆ exhibited some distortions: (a) the internal Au atom in each Au₁₁ unit was closer to the apex and equatorial Au atoms than to the four Au atoms at the interface of the two units (2.63-2.67 Å vs 2.70-2.90 Å); (b) the apex Au atom was pulled closer to one side of the equatorial Au atoms (3.05-3.16 Å vs 3.52-3.63 Å) due to the coordination of the bidentate L⁸ ligand. The UV-vis absorption spectrum of Au₂₂(L⁸)₆ was also different from the undecagold [Au₁₁]³⁺, for which all surface Au atoms were coordinated. 45,46

It was also remarkable that the new $\mathrm{Au}_{22}(\mathrm{L}^8)_6$ AuNC was neutral with a 22-electron core, which did not obey the major shell-closing in the electron-shell model. As mentioned above and shown in the detailed structure of the Au_{22} core (Figure 5c), the Au–Au bonding between the two Au_{11} units was strong, and it could not be viewed simply as a dimer of undecagold. A subsequent theoretical study showed that the molecular orbitals in the Au_{22} core were delocalized on both Au_{11} units, so implying that Au_{22} should be viewed as a new and integrated cluster entity. The computed HOMO–LUMO gap for $\mathrm{Au}_{22}(\mathrm{L}^8)_6$ was 0.9 eV, but the HOMO \rightarrow LUMO transition was forbidden, so in agreement with the experimental UV–vis absorption spectrum with a strong peak at 2.4 eV and a long tail into the red.

5. POLYMORPHISM OF THE PHOSPHINE-PROTECTED Au_{22} CLUSTER

After exploring the influence of diphosphine-ligand chain lengths on the nuclearity and shape of AuNCs, we also studied the effect of the chain rigidity using bis(2-diphenylphosphino)-ethyl ether (dppee) (inset in Figure 6). The O atom in the

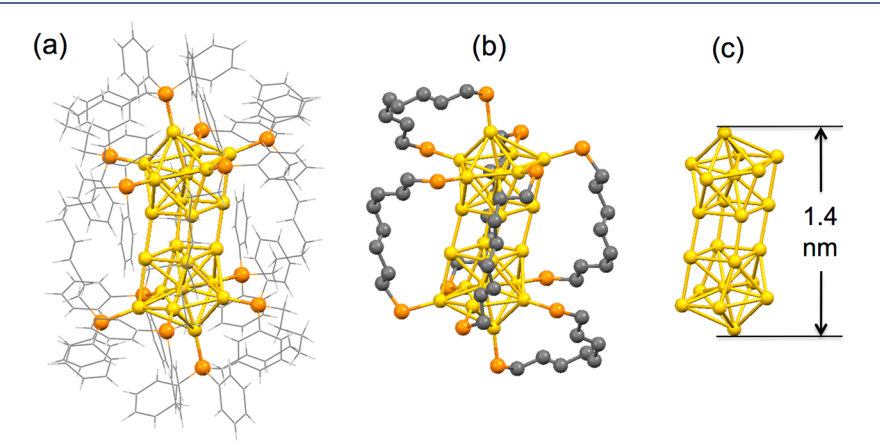


Figure 5. (a) Crystal structure of $Au_{22}(L^8)_6$. (b) Structure of $Au_{22}(L^8)_6$ showing only the carbon backbones of the L^8 ligands. (c) The Au_{22} core structure of $Au_{22}(L^8)_6$. Yellow = Au, orange = P, gray = C. Reproduced with permission from ref 38. Copyright 2014 American Chemical Society.

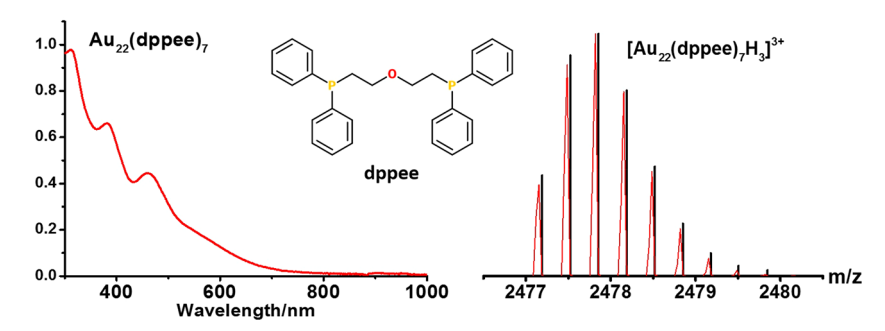


Figure 6. UV—vis absorption spectrum of the $Au_{22}(dppee)_7$ nanocluster (left) and the observed (red) and simulated (black) isotopic patterns of the $[Au_{22}(dppee)_7H_3]^{3+}$ ion in ESI-MS. The inset shows the structure of the dppee ligand. Reproduced with permission from ref 40. Copyright 2016 Wiley-VCH Verlag GmbH & Co.

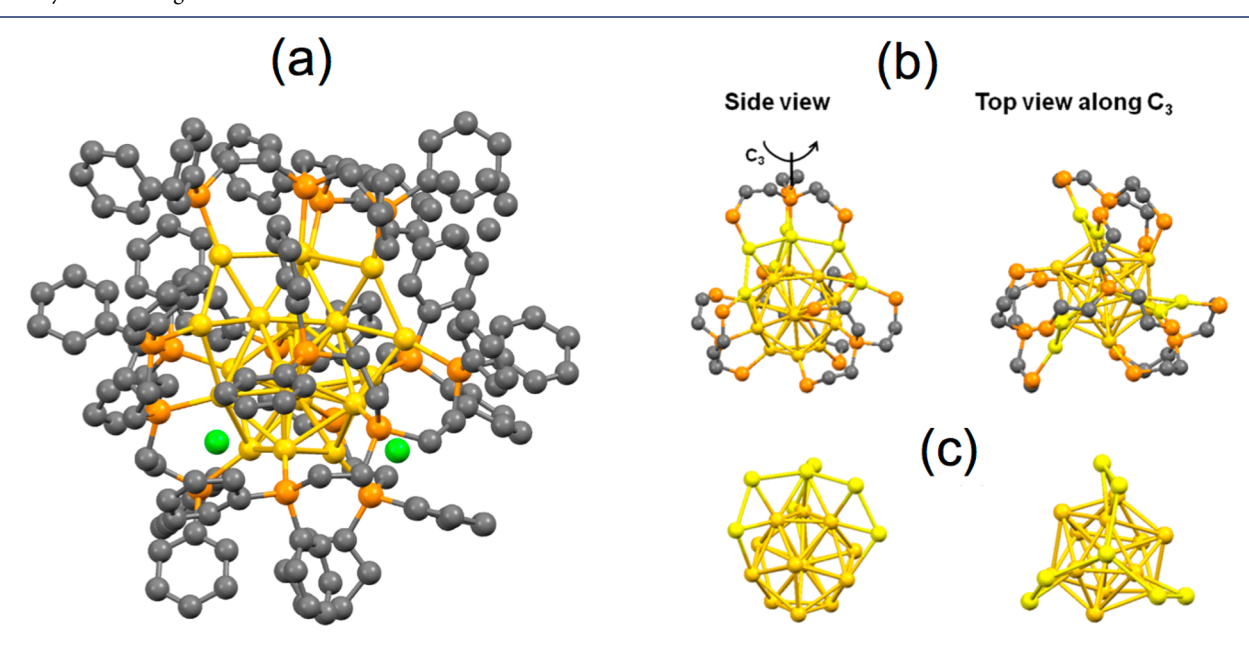


Figure 7. (a) Structure of $Au_{20}(PP_3)_4Cl_4$ (color labels: gold = Au; orange = P; gray = C; green = Cl; H atoms are omitted). (b) Structure of $Au_{20}(PP_3)_4Cl_4$ showing only the C backbone of the PP_3 ligands. (c) Au_{20} core of $Au_{20}(PP_3)_4Cl_4$. Reproduced with permission from ref 39. Copyright 2014 American Chemical Society.

carbon chain increased the flexibility of the ligand, making it possible to chelate larger Au_N cores than the L⁵ ligand (similar chain length). With the L5 ligand, we observed high abundances of $Au_8(L^5)_4^{2+}$ and $Au_{10}(L^5)_4^{2+}$ previously.³⁷ As expected, a high-nuclearity AuNC with a formula of Au₂₂(dppee)₇ was observed when the Cl₂Au₂(dppee) precursor was reduced by NaBH₄. 40 The temperature-dependent yield and the slow decomposition of the purified product in solution suggested a kinetically controlled reaction in the formation of the new Au₂₂(dppee)₇ nanocluster. ESI-MS showed a clean spectrum with three protons, $[Au_{22}(dppee)_7H_3]^{3+}$ (Figure 6, right). The UV-vis absorption spectrum displayed three distinct peaks at 460, 380, and 310 nm (Figure 6, left), which were different from that of Au₂₂(L⁸)₆, 38 suggesting that the two Au₂₂ nanoclusters with different diphosphine ligands had different shapes and structures. Further MS/MS and ³¹P NMR characterizations provided more information about the structural differences and relationships between the Au₂₂ cores in Au₂₂(dppee)₇ and $Au_{22}(L^8)_6$. Although the exact structure of $Au_{22}(dppee)_7$ was not solved due to the challenges of single-crystal growth, the spectroscopic studies suggested a core structure consisting of a Au₁₁ unit with the remaining 11 Au atoms bonded to its

perimeter. The $Au_{22}(dppee)_7$ nanocluster provided a new example of ligand effects on the nuclearity and structural polymorphism of phosphine-protected AuNC. It further validated our strategy to use different diphosphine ligands to control the size and shape of AuNCs as a guiding principle to search for large-scale synthesis of the T_d -Au₂₀.

PHOSPHINE-PROTECTED NONTETRAHEDRAL Au₂₀ NANOCLUSTERS

Based on the coordination geometry of the L⁸ diphosphine ligand in $\mathrm{Au}_{22}(\mathrm{L}^8)_6$ (Figure 5), we surmised that a more flexible and multidentate ligand might be necessary to capture the T_d -Au₂₀. This idea led to our consideration of the commercially available tetraphosphine ligand, tris[2-(diphenylphosphino)ethyl]phosphine (PP₃). We hypothesized that the 3-fold symmetry of PP₃ might match the C_3 -axis of the tetrahedral Au₂₀. We again prepared the $\mathrm{Cl}_4\mathrm{Au}_4\mathrm{PP}_3$ precursor from ClAuPPh₃ and reduced it with NaBH₄ in a dichloromethane solution. We were excited to obtain a $[\mathrm{Au}_{20}(\mathrm{PP}_3)_4]^{4+}$ nanocluster readily using ESI-MS. We were initially confident that our long-sought T_d -Au₂₀ had finally been synthesized. However, when the crystal structure was solved, we were really stupefied that the Au₂₀ core in $[\mathrm{Au}_{20}(\mathrm{PP}_3)_4]\mathrm{Cl}_4$ had a

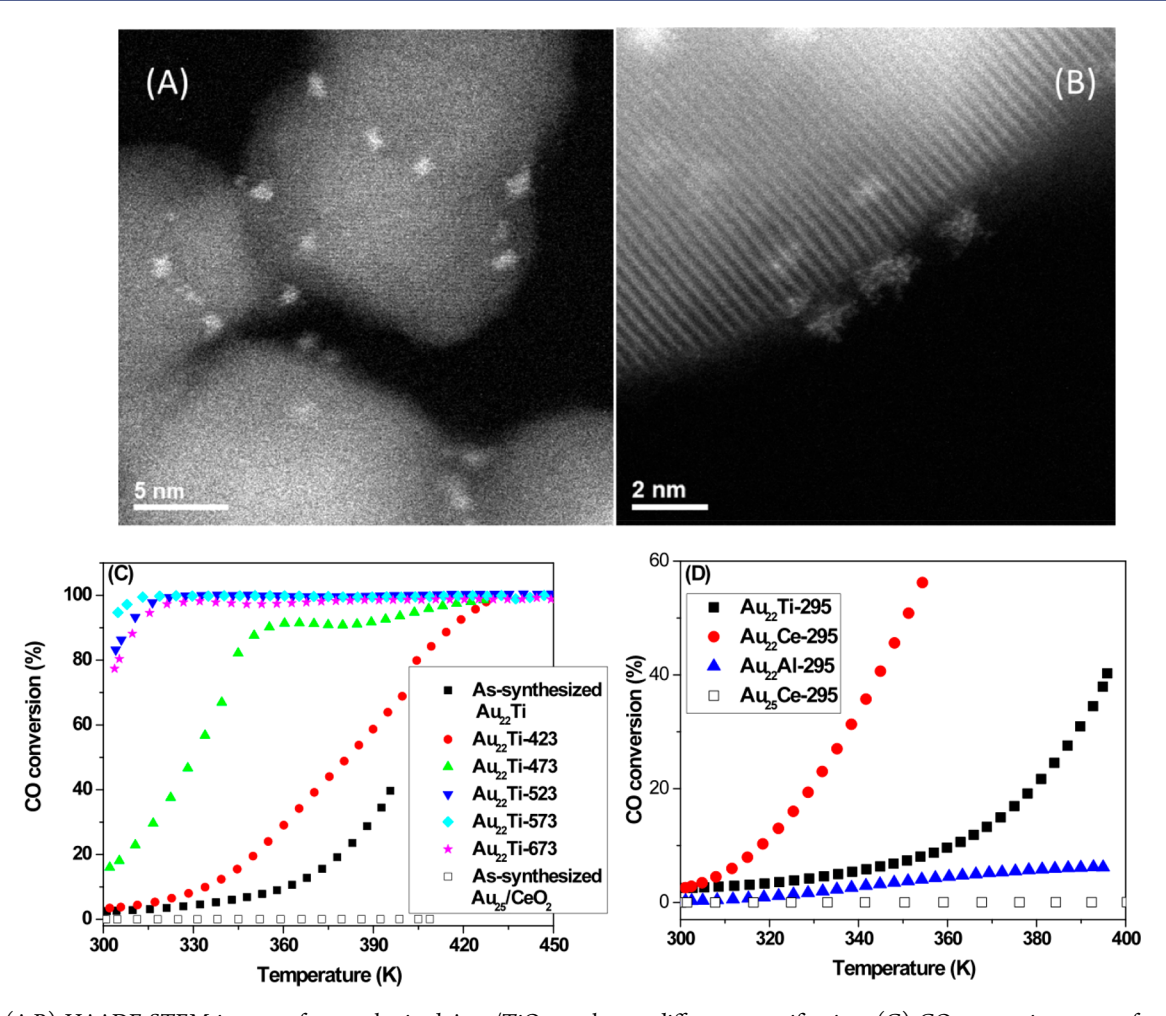


Figure 8. (A,B) HAADF-STEM images of as-synthesized Au_{22}/TiO_2 catalyst at different magnification. (C) CO conversion curves for the Au_{22}/TiO_2 catalyst pretreated in O_2 at different temperatures. (D) CO conversion curves for different as-synthesized AuNC/oxide catalysts. Reproduced with permission from ref 41. Copyright 2016 American Chemical Society.

completely different structure than we expected (Figure 7). The new Au₂₀ cluster was found to consist of an icosahedraltype Au₁₃ core with a seven-atom second Au layer arranged in a propeller fashion (Figure 7c), giving rise to an intrinsically chiral AuNC. In fact, all 16 surface atoms in the chiral Au₂₀ core were coordinated, resulting in a very stable cluster. We also found that the [Au₂₀(PP₃)₄]Cl₄ nanoclusters could be synthesized with quite high yields, ~50% based on Au atoms. It should be pointed out that the same [Au₂₀(PP₃)₄]Cl₄ cluster was also reported independently by Wan et al. at a slightly lower yield.⁵⁷ The electronic structure of [Au₂₀(PP₃)₄]Cl₄ was investigated by DFT calculations.⁵⁸ A large HOMO-LUMO gap of 1.30 eV was found, in agreement with its high stability. The second-order nonlinear optical properties of [Au₂₀(PP₃)₄]Cl₄ have also been investigated.⁵⁹ During the review of this Account, a report on the enantioseparation of the chiral [Au₂₀(PP₃)₄]Cl₄ clusters has appeared.⁶⁰

Besides the chiral Au_{20} core in $[\mathrm{Au}_{20}(\mathrm{PP}_3)_4]\mathrm{Cl}_4$, an achiral Au_{20} core was reported previously using mixed ligands of bis(2-pyridyl)-phenylphosphine (PPhPy₂) and chloride, $[\mathrm{Au}_{20}(\mathrm{PPhPy}_2)_{10}\mathrm{Cl}_6]$, or more recently with mixed ligands of bis(diphenylphosphino)methane (dppm) and cyanide, $[\mathrm{Au}_{20}(\mathrm{dppm})_6(\mathrm{CN})_6]$. The structure of the achiral Au_{20} core was elongated and could be viewed as the fusion of two

 Au_{11} cluster sharing two vertices. The electronic structure and stability of the achiral $\left[Au_{20}\right]^{6+}$ core was studied theoretically.⁶³

7. CATALYSES OF Au₂₂(L⁸)₆: IMPORTANCE OF THE UNCOORDINATED GOLD AS *IN SITU* CATALYTICALLY ACTIVE SITES

The Au₂₂(L⁸)₆ nanocluster with uncoordinated Au sites provided an unprecedented opportunity to study catalytic reactions on well-defined active sites with truly atomic precision. The aliphatic chains around the uncoordinated Au atoms in $Au_{22}(L^8)_6$ were not expected to hinder access of small molecules to these in situ activation centers. Wu et al. carried out an extensive investigation of CO oxidation by the Au₂₂(L⁸)₆ nanocluster dispersed on different oxide supports (i.e., Al₂O₃, TiO₂, or CeO₂).⁴¹ Figure 8A,B shows that the Au₂₂(L⁸)₆ nanoclusters were well dispersed on the TiO₂ support without aggregation. The intact metal-ligand coordination environment was confirmed by extended X-ray absorption fine structure (EXAFS) spectroscopy and IR spectroscopy. The as-prepared Au₂₂(L⁸)₆ catalyst showed a small but detectable CO conversion to CO2 on reducible supports (TiO₂ and CeO₂), even at room temperature (Figure 8D). This observation was completely different from the assynthesized CeO₂-supported thiolate-protected Au₂₅(SR)₁₈ nanoclusters, where no CO oxidation was detected at room

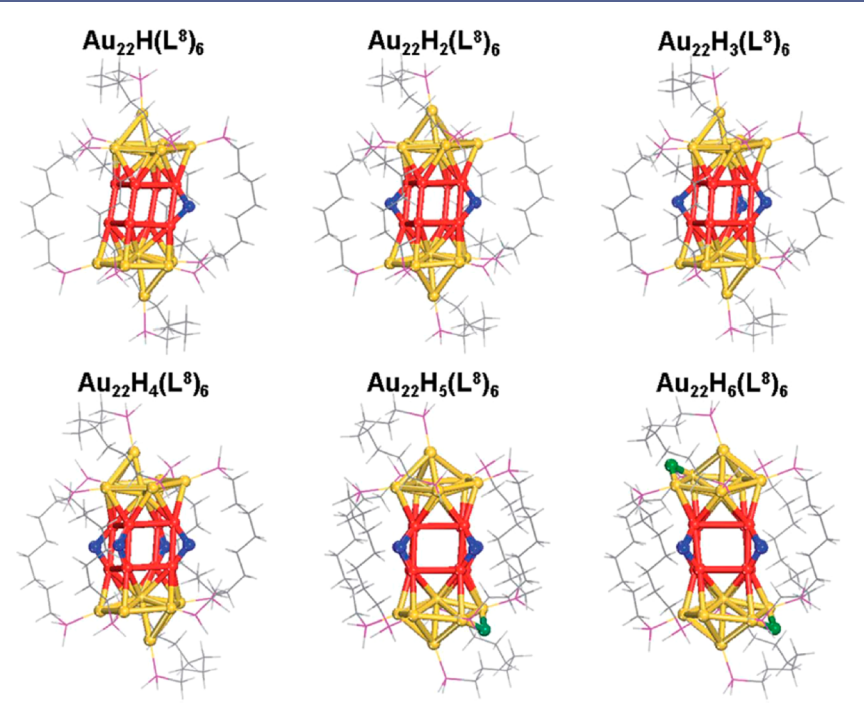


Figure 9. Structures of the $Au_{22}H_n(L^8)_6$ clusters for n = 1-6. The uncoordinated Au atoms are in red, and the H atoms are in blue and green. Reproduced with permission from ref 43. Copyright 2018 The Royal Society of Chemistry.

temperature, ⁴¹ because Au₂₅(SR)₁₈ did not contain any uncoordinated sites. ^{64,65} Another intriguing observation was that no obvious CO oxidation occurred at room temperature on the Al₂O₃ support, suggesting a different mechanism on the nonreducible oxide. At elevated temperatures, all as-synthesized Au₂₂/oxide catalysts showed higher reactivity for CO oxidation, even for the Al₂O₃ support (Figure 8D). At any given temperature, the more reducible supports displayed higher activities (CeO₂ > TiO₂ > Al₂O₃). For comparison, the as-synthesized Au₂₅(SR)₁₈/CeO₂ sample did not exhibit any CO oxidation even at above 400 K (Figure 8D).

The thermal stability of the $Au_{22}(L^8)_6$ /oxide catalysts was characterized by TGA, EXAFS, and IR spectroscopy. It was found that the Au₂₂(L⁸)₆ cluster was stable up to 523 K, above which ligand dissociation occurred. 41 The activity of the $Au_{22}(L^8)_6$ /oxide catalyst was found to depend on the thermal treatment of the sample, even below the ligand dissociation temperature, as shown in Figure 8C for the Au₂₂(L⁸)₆/TiO₂ catalyst. The activity increased as the treatment temperature increased, saturating above the ligand dissociation temperature of 523 K. The catalytic mechanisms of CO oxidation were further investigated using the ¹⁸O₂ isotope. ⁴¹ It was found that the Mars-van Krevelen pathway (CO absorbed on AuNC active sites, O comes from the oxide support) was dominant on the reducible oxide supports (TiO₂ and CeO₂), while the Langmuir-Hinshelwood (both CO and O2 were absorbed on the AuNC sites) dominated on the nonreducible support

The shapes of the oxide support on the catalytic activity of the $\mathrm{Au}_{22}(\mathrm{L}^8)_6$ nanocluster were also investigated for CO oxidation. Two types of CeO_2 particles with different morphologies, rod-like and cube-like, were used to prepare the $\mathrm{Au}_{22}(\mathrm{L}^8)_6/\mathrm{CeO}_2$ catalyst. It was found that the $\mathrm{Au}_{22}(\mathrm{L}^8)_6/\mathrm{CeO}_2$ -rod sample displayed higher activities than the $\mathrm{Au}_{22}(\mathrm{L}^8)_6/\mathrm{CeO}_2$ -cube sample. These different catalysts were also characterized by EXAFS, HAADF-STEM, and *in situ* IR

spectroscopy. It was found that the lattice oxygen atoms in the CeO_2 -rod support were much more reactive than those in the CeO_2 -cube support, leading to the much faster oxidation of chemisorbed CO on the $Au_{22}(L^8)_6/CeO_2$ -rod catalyst.⁴²

Besides CO oxidation, theoretical calculations suggested that the $\mathrm{Au}_{22}(\mathrm{L}^8)_6$ nanocluster could activate H_2 even better than Pt, thereby being a potentially promising catalyst for the hydrogen evolution reaction. The was found that up to six H atoms can adsorb onto the $\mathrm{Au}_{22}(\mathrm{L}^8)_6$ cluster, as shown in Figure 9. In addition to providing six H adsorption sites per cluster, the Gibbs energy for each H adsorption on $\mathrm{Au}_{22}(\mathrm{L}^8)_6$ was close to zero at room temperature, suggesting that the H adsorption would be reversible. The second hydrogen atom was found to exhibit the strongest binding energy (-0.41 eV), indicating that the $\mathrm{Au}_{22}\mathrm{H}_2(\mathrm{L}^8)_6$ dihydride cluster might be isolable.

8. CONCLUSIONS AND PERSPECTIVES

The discovery of the highly stable T_d -Au₂₀ cluster in the gas phase has inspired exploratory efforts toward its large-scale solution syntheses, so that its interesting optical and catalytic properties may be exploited and harnessed. Phosphine ligands were selected, in order to keep the tetrahedral structure of this unique gold pyramid, which has the bulk atomic arrangement with all its atoms on the surface. The prospect of preparing ligated T_d -Au₂₀ with uncoordinated Au sites as in situ catalytic centers is very attractive, providing the ultimate atomically precise models to help elucidate the catalytic mechanisms of nanogold. 66,67 Although the ultimate goal has not been reached, the adventure has already yielded some exciting results. In particular, the first AuNC with uncoordinated sites using a diphosphine ligand, Au₂₂(L⁸)₆, has been synthesized and found to exhibit in situ catalytic activities for CO oxidation and H₂ activation. Furthermore, the chemistry of phosphineprotected AuNCs has been expanded and enriched, leading to the syntheses of the first intrinsically chiral gold nanocluster

using a tetradentate-ligand, [Au₂₀(PP₃)₄]Cl₄. In terms of synthetic conditions, the reducing agent or solvents may be controlled to yield different clusters. For example, the popular NaBH₄ reducing agent may be replaced by the milder NaB₃H₈, which has become more readily available through a recent facile synthetic method.⁶⁸ There are also unlimited opportunities to tune the phosphine ligands, as demonstrated by the recent synthesis of enantiopure phosphine-protected Au₂₄ clusters when enantiopure diphosphine ligands were used.⁶⁹ It is expected that with the proper ligands and the right synthetic conditions the Au₂₀ pyramid should be within reach. Regardless, phosphine-protected AuNCs have been demonstrated to be a rich area of research, and many new and exciting atomically precise clusters are expected to be discovered.

AUTHOR INFORMATION

Corresponding Author

*E-mail: lai-sheng_wang@brown.edu.

ORCID ®

Qian-Fan Zhang: 0000-0002-6493-5505 Xuenian Chen: 0000-0001-9029-1777 Lai-Sheng Wang: 0000-0003-1816-5738

Notes

The authors declare no competing financial interest.

Biographies

Qian-Fan Zhang received his B.S. and M.S. degrees from Wuhan University in China. He is currently a Ph.D. student in Prof. Lai-Sheng Wang's group at Brown University focusing on the synthesis, characterization, and application of gold and boron related nanomaterials.

Xuenian Chen received his B.S. and M.S. degrees from Lanzhou University in China and his Ph.D. from Lanzhou Institute of Chemical Physics, Chinese Academy of Sciences. He did postdoctoral work and then became Research Scientist at the Department of Chemistry and the Department of Materials Science at The Ohio State University. He is currently Distinguished Professor in the School of Chemistry and Chemical Engineering at Henan Normal University, Xinxiang, China. His research interests are in boron chemistry, organometallics, catalysis, and materials science.

Lai-Sheng Wang is currently the Jesse H. and Louisa D. Sharpe Metcalf Professor of Chemistry at Brown University. He received his B.S. degree from Wuhan University and his Ph.D. from the University of California at Berkeley. His research group focuses on the investigation of the fundamental behaviors of nanoclusters using photoelectron spectroscopy and imaging. His group has also developed electrospray and cryogenic ion trap techniques for the spectroscopic studies of free multiply charged anions and complex solution molecules in the gas phase.

ACKNOWLEDGMENTS

The work was supported by the National Science Foundation (Grant DMR-1655066 to L.S.W.) and the National Natural Science Foundation of China (Grant Nos. 21771057 and 21371051 to X.N.C.). The authors thank Jing Chen for her contributions to the syntheses of the phosphine-protected gold nanoclusters and Zili Wu and De-en Jiang for collaboration on the investigation of the catalytic properties of the Au₂₂ cluster.

REFERENCES

- (1) Daniel, M. C.; Astruc, D. Gold Nanoparticles: Assembly, Supramolecular Chemistry, Quantum-Size-Related Properties, and Applications toward Biology, Catalysis, and Nanotechnology. *Chem. Rev.* **2004**, *104*, 293–346.
- (2) Giljohann, D. A.; Seferos, D. S.; Daniel, W. L.; Massich, M. D.; Patel, P. C.; Mirkin, C. A. Gold Nanoparticles for Biology and Medicine. *Angew. Chem., Int. Ed.* **2010**, *49*, 3280–3294.
- (3) Taylor, K. J.; Pettiettehall, C. L.; Cheshnovsky, O.; Smalley, R. E. Ultraviolet Photoelctron Spectra of Coinage Metal Clusters. *J. Chem. Phys.* **1992**, *96*, 3319–3329.
- (4) Zhai, H. J.; Li, X.; Wang, L. S. Probing the Unique Size-Dependent Properties of Small Au Clusters, Au Alloy Clusters, and CO-Chemisorbed Au Clusters in the Gas Phase. In *The Chemical Physics of Solid Surfaces*; Woodruff, D. P., Ed.; Elsevier: 2007; Vol. 12, pp 91–150.
- (5) Wang, L. M.; Wang, L. S. Probing the Electronic Properties and Structural Evolution of Anionic Gold Clusters in the Gas Phase. *Nanoscale* **2012**, *4*, 4038–4053.
- (6) Gilb, S.; Weis, P.; Furche, F.; Ahlrichs, R.; Kappes, M. M. Structures of Small Gold Cluster Cations (Au^{n+} , n < 14): Ion Mobility Measurements versus Density Functional Calculations. *J. Chem. Phys.* **2002**, *116*, 4094–4101.
- (7) Furche, F.; Ahlrichs, R.; Weis, P.; Jacob, C.; Gilb, S.; Bierweiler, T.; Kappes, M. M. The Structures of Small Gold Cluster Aions as Determined by a Combination of Ion Mobility Measurements and Density Functional Calculations. *J. Chem. Phys.* **2002**, *117*, 6982–6990.
- (8) Häkkinen, H.; Yoon, B.; Landman, U.; Li, X.; Zhai, H. J.; Wang, L. S. On the Electronic and Atomic Structures of Small $\mathrm{Au_{N}}^{-}$ (N = 4–14) Clusters: A Photoelectron Spectroscopy and Density-Functional Study. *J. Phys. Chem. A* **2003**, *107*, 6168–6175.
- (9) Li, J.; Li, X.; Zhai, H. J.; Wang, L. S. Au₂₀: A Tetrahedral Cluster. *Science* **2003**, 299, 864–867.
- (10) Bulusu, S.; Li, X.; Wang, L. S.; Zeng, X. C. Evidence of Hollow Golden Cages. *Proc. Natl. Acad. Sci. U. S. A.* **2006**, *103*, 8326–8330.
- (11) Xing, X. P.; Yoon, B.; Landman, U.; Parks, J. H. Structural Evolution of Au Nanoclusters: From Planar to Cage to Tubular Motifs. *Phys. Rev. B: Condens. Matter Mater. Phys.* **2006**, 74, 165423.
- (12) Bulusu, S.; Li, X.; Wang, L. S.; Zeng, X. C. Structural Transition from Pyramidal to Space-Filling Amorphous in Medium-Sized Gold Clusters: Au_n^- (n=21-25). *J. Phys. Chem. C* **2007**, *111*, 4190–4198.
- (13) Huang, W.; Ji, M.; Dong, C. D.; Gu, X.; Wang, L. M.; Gong, X. G.; Wang, L. S. Relativistic Effects and the Unique Low-Symmetry Structures of Gold Nanoclusters. *ACS Nano* **2008**, *2*, 897–904.
- (14) Huang, W.; Bulusu, S.; Pal, R.; Zeng, X. C.; Wang, L. S. Structural Transition of Gold Nanoclusters: From the Golden Cage to the Golden Pyramid. *ACS Nano* **2009**, *3*, 1225–1230.
- (15) Schooss, D.; Weis, P.; Hampe, O.; Kappes, M. M. Determining the Size-Dependent Structure of Ligand-Free Gold-Cluster Ions. *Philos. Trans. R. Soc., A* **2010**, 368, 1211–1243.
- (16) Huang, W.; Pal, R.; Wang, L. M.; Zeng, X. C.; Wang, L. S. Isomer Identification and Resolution in Small Gold Clusters. *J. Chem. Phys.* **2010**, *132*, 054305.
- (17) Shao, N.; Huang, W.; Gao, Y.; Wang, L. M.; Li, X.; Wang, L. S.; Zeng, X. C. Probing the Structural Evolution of Medium-Sized Gold Clusters: Au_n^- (n=27 to 35). *J. Am. Chem. Soc.* **2010**, 132, 6596–6605.
- (18) Shao, N.; Huang, W.; Mei, W.-N.; Wang, L. S.; Wu, Q.; Zeng, X. C. Structural Evolution of Medium-Sized Gold Clusters Au_n^- (n=36,37,38): Appearance of Bulk-Like Face Centered Cubic Fragment. *J. Phys. Chem. C* **2014**, *118*, 6887–6892.
- (19) Schaefer, B.; Pal, R.; Khetrapal, N. S.; Amsler, M.; Sadeghi, A.; Blum, V.; Zeng, X. C.; Goedecker, S.; Wang, L. S. Isomerism and Structural Fluxionality in the Au₂₆ and Au₂₆⁻ Nanoclusters. *ACS Nano* **2014**, *8*, 7413–7422.
- (20) Pande, S.; Huang, W.; Shao, N.; Wang, L.-M.; Khetrapal, N.; Mei, W. N.; Jian, T.; Wang, L. S.; Zeng, X. C. Structural Evolution of

Core-Shell Gold Nanoclusters: Au_n^- (n = 42-50). ACS Nano 2016, 10, 10013-10022.

- (21) Landman, U.; Yoon, B.; Zhang, C.; Heiz, U.; Arenz, M. Factors in Gold Nanocatalysis: Oxidation of CO in the Non-Scalable Size Regime. *Top. Catal.* **2007**, *44*, 145–158.
- (22) Gruene, P.; Rayner, D. M.; Redlich, B.; van der Meer, A. F. G.; Lyon, J. T.; Meijer, G.; Fielicke, A. Structures of Neutral Au₇, Au₁₉, and Au₂₀ Clusters in the Gas Phase. *Science* **2008**, 321, 674–676.
- (23) Wang, Z. W.; Palmer, R. E. Direct Atomic Imaging and Dynamical Fluctuations of the Tetrahedral Au₂₀ Cluster. *Nanoscale* **2012**, *4*, 4947–4949.
- (24) Molina, L. M.; Hammer, B. The Activity of the Tetrahedral Au₂₀ Cluster: Charging and Impurity Effect. *J. Catal.* **2005**, 233, 399–404.
- (25) Li, Z.; Chen, Z. X.; He, X.; Kang, G. J. Theoretical Studies of Acrolein Hydrogenation on Au₂₀ Nanoparticle. *J. Chem. Phys.* **2010**, 132, 184702.
- (26) Bobuatong, K.; Karanjit, S.; Fukuda, R.; Ehara, M.; Sakurai, H. Aerobic Oxidation of Methanol to Formic Acid on Au₂₀⁻: A Theoretical Study on the Reaction Mechanism. *Phys. Chem. Chem. Phys.* **2012**, *14*, 3103–3111.
- (27) Hull, J. M.; Provorse, M. R.; Aikens, C. M. Formyloxyl Radical-Gold Nanoparticle Binding: A Theoretical Study. *J. Phys. Chem. A* **2012**, *116*, 5445–5452.
- (28) Pal, R.; Wang, L. M.; Pei, Y.; Wang, L. S.; Zeng, X. C. Unraveling the Mechanisms of O_2 Activation by Size-Selected Gold Clusters: Transition from Superoxo to Peroxo Chemisorption. *J. Am. Chem. Soc.* **2012**, *134*, 9438–9445.
- (29) Beletskaya, A. V.; Pichugina, D. A.; Shestakov, A. F.; Kuz'menko, N. E. Formation of H₂O₂ on Au₂₀ and Au₁₉Pd Clusters: Understanding the Structure Effect on the Atomic Level. *J. Phys. Chem. A* **2013**, *117*, 6817–6826.
- (30) Lin, S.; Pei, Y. Mechanistic Insight into the Styrene-Selective Oxidation on Subnanometer Gold Clusters (Au₁₆–Au₂₀, Au₂₇, Au₂₈, Au₃₀, and Au₃₂–Au₃₅): A Density Functional Theory Study. *J. Phys. Chem. C* **2014**, *118*, 20346–20356.
- (31) Wang, Y.-G.; Cantu, D. C.; Lee, M. S.; Li, J.; Glezakou, V. A.; Rousseau, R. CO Oxidation on Au/TiO₂: Condition-Dependent Active Sites and Mechanistic Pathways. *J. Am. Chem. Soc.* **2016**, *138*, 10467–10476.
- (32) Wu, K. H.; Li, J.; Lin, C. S. Remarkable Second-Order Optical Nonlinearity of Nano-Sized Au₂₀ Cluster: A TDDFT Study. *Chem. Phys. Lett.* **2004**, 388, 353–357.
- (33) Aikens, C. M.; Schatz, G. C. TDDFT Studies of Absorption and SERS Spectra of Pyridine Interacting with Au₂₀. *J. Phys. Chem. A* **2006**, *110*, 13317–13324.
- (34) Kryachko, E. S.; Remacle, F. The Magic Cluster Au₂₀. *Int. J. Quantum Chem.* **2007**, 107, 2922–2934.
- (35) Yu, C.; Harbich, W.; Sementa, L.; Ghiringhelli, L.; Aprá, E.; Stener, M.; Fortunelli, A.; Brune, H. Intense fluorescence of Au₂₀. *J. Chem. Phys.* **2017**, *147*, 074301.
- (36) Zhang, H. F.; Stender, M.; Zhang, R.; Wang, C. M.; Li, J.; Wang, L. S. Toward the Solution Synthesis of the Tetrahedral Au₂₀ Cluster. *J. Phys. Chem. B* **2004**, *108*, 12259–12263.
- (37) Bertino, M. F.; Sun, Z. M.; Zhang, R.; Wang, L. S. Facile Syntheses of Monodisperse Ultrasmall Au Clusters. *J. Phys. Chem. B* **2006**, *110*, 21416–21418.
- (38) Chen, J.; Zhang, Q. F.; Bonaccorso, T. A.; Williard, P. G.; Wang, L. S. Controlling Gold Nanoclusters by Diphospine Ligands. *J. Am. Chem. Soc.* **2014**, *136*, 92–95.
- (39) Chen, J.; Zhang, Q.-F.; Williard, P. G.; Wang, L. S. Synthesis and Structure Determination of a New Au₂₀ Nanocluster Protected by Tripodal Tetraphosphine Ligands. *Inorg. Chem.* **2014**, *53*, 3932–3934.
- (40) Zhang, Q. F.; Williard, P. G.; Wang, L. S. Polymorphism of Phosphine-Protected Gold Nanoclusters: Synthesis and Characterization of a New 22-Gold-Atom Cluster. *Small* **2016**, *12*, 2518–2525.
- (41) Wu, Z.; Hu, G.; Jiang, D.-e.; Mullins, D. R.; Zhang, Q. F.; Allard, L. F.; Wang, L. S.; Overbury, S. H. Diphosphine-Protected

Au₂₂ Nanoclusters on Oxide Supports Are Active for Gas-Phase Catalysis without Ligand Removal. *Nano Lett.* **2016**, *16*, 6560–6567.

- (42) Wu, Z.; Mullins, D. R.; Allard, L. F.; Zhang, Q.; Wang, L. CO Oxidation Over Ceria Supported Au₂₂ Nanoclusters: Shape Effect of the Support. *Chin. Chem. Lett.* **2018**, 29, 795–799.
- (43) Hu, G.; Wu, Z.; Jiang, D.-e. Stronger-Than-Pt Hydrogen Adsorption in a Au₂₂ Aanocluster for the Hydrogen Evolution Reaction. *J. Mater. Chem. A* **2018**, *6*, 7532–7537.
- (44) Jin, R.; Zeng, C.; Zhou, M.; Chen, Y. Atomically Precise Colloidal Metal Nanoclusters and Nanoparticles: Fundamentals and Opportunities. *Chem. Rev.* **2016**, *116*, 10346–10413.
- (45) Bellon, P.; Sansoni, M.; Manassero, M. Crystal and Molecular Structure of Tri-Iodoheptakis(Tri-Para-Fluorophenyl-Phosphine)-Undecagold. *J. Chem. Soc., Dalton Trans.* **1972**, 1481–1482.
- (46) Bartlett, P. A.; Bauer, B.; Singer, S. J. Synthesis of Water-Soluble Undecagold Cluster Coomounds of Potential Imporance in Electron-Microscopi and Other Studies of Biological-Systems. *J. Am. Chem. Soc.* **1978**, *100*, 5085–5089.
- (47) Briant, C. E.; Theobald, B. R. C.; White, J. W.; Bell, L. K.; Mingos, D. M. P.; Welch, A. J. Synthesis and X-Ray Structural Characterization of the Centered Icosahedral Gold Cluster Compound $[Au_{13}(PME_2Ph)_{10}Cl_2](PF_6)_3$ The Realziation of a Theoretical Prediction. J. Chem. Soc., Chem. Commun. 1981, 201–202.
- (48) Hall, K. P.; Mingos, D. M. P. Homonuclaer and Heteronuclear Cluster Compounds of Gold. *Prog. Inorg. Chem.* **2007**, 32, 237–325. (49) Shichibu, Y.; Konishi, K. HCl-Induced Nuclearity Convergence
- in Diphosphine-Protected Ultrasmall Gold Clusters: A Novel Synthetic Route to "Magic-Number" Au₁₃ Clusters. Small **2010**, 6, 1216–1220.
- (50) Konishi, K. Phosphine-Coordinated Pure-Gold Clusters: Diverse Geometrical Structures and Unique Optical Properties/Responses. In *Gold Clusters, Colloids and Nanoparticles I*; Mingos, D. M. P., Ed.; Springer International Publishing: Cham, 2014; pp 49–86.
- (51) Weare, W. W.; Reed, S. M.; Warner, M. G.; Hutchison, J. E. Improved Synthesis of Small ($d_{CORE} \approx 1.5$ nm) Phosphine-Stabilized Gold Nanoparticles. *J. Am. Chem. Soc.* **2000**, 122, 12890–12891.
- (52) Pettibone, J. M.; Hudgens, J. W. Gold Cluster Formation with Phosphine Ligands: Etching as a Size-Selective Synthetic Pathway for Small Clusters? *ACS Nano* **2011**, *5*, 2989–3002.
- (53) Hudgens, J. W.; Pettibone, J. M.; Senftle, T. P.; Bratton, R. N. Reaction Mechanism Governing Formation of 1,3-Bis-(diphenylphosphino)propane-Protected Gold Nanoclusters. *Inorg. Chem.* **2011**, *50*, 10178–10189.
- (54) Pettibone, J. M.; Hudgens, J. W. Reaction Network Governing Diphosphine-Protected Gold Nanocluster Formation from Nascent Cationic Platforms. *Phys. Chem. Chem. Phys.* **2012**, *14*, 4142–4154.
- (55) Walter, M.; Akola, J.; Lopez-Acevedo, O.; Jadzinsky, P. D.; Calero, G.; Ackerson, C. J.; Whetten, R. L.; Grönbeck, H.; Häkkinen, H. A Unified View of Ligand-Protected Gold Clusters as Superatom Complexes. *Proc. Natl. Acad. Sci. U. S. A.* **2008**, *105*, 9157–9162.
- (56) Muniz-Miranda, F.; Presti, D.; Menziani, M. C.; Pedone, A. Electronic and Optical Properties of the Au₂₂[1,8-bis-(diphenylphosphino)octane]₆ Nanoclusters Disclosed by DFT and TD-DFT Calculations. *Theor. Chem. Acc.* **2016**, 135, 5.
- (57) Wan, X. K.; Yuan, S. F.; Lin, Z. W.; Wang, Q. M. A Chiral Gold Nanocluster Au₂₀ Protected by Tetradentate Phosphine Ligands. *Angew. Chem., Int. Ed.* **2014**, *53*, 2923–2926.
- (58) Knoppe, S.; Lehtovaara, L.; Häkkinen, H. Electronic Structure and Optical Properties of the Intrinsically Chiral 16-Electron Superatom Complex [Au₂₀(PP₃)₄]⁴⁺. *J. Phys. Chem. A* **2014**, *118*, 4214–4221.
- (59) Knoppe, S.; Zhang, Q. F.; Wan, X. K.; Wang, Q. M.; Wang, L. S.; Verbiest, T. Second-Order Nonlinear Optical Scattering Properties of Phosphine-Protected Au₂₀ Clusters. *Ind. Eng. Chem. Res.* **2016**, 55, 10500–10506.
- (60) Zhu, Y.; Wang, H.; Wan, K.; Guo, J.; He, C.; Yu, Y.; Zhao, L.; Zhang, Y.; Lv, J.; Shi, L.; Jin, R.; Zhang, X.; Shi, X.; Tang, Z. Enantioseparation of $\mathrm{Au}_{20}(\mathrm{PP}_3)_4\mathrm{Cl}_4$ clusters of intrinsic core chirality. *Angew. Chem., Int. Ed.* **2018**, *57*, 9059.

(61) Wan, X. K.; Lin, Z. W.; Wang, Q. M. Au₂₀ Nanocluster Protected by Hemilabile Phosphines. *J. Am. Chem. Soc.* **2012**, *134*, 14750–14752.

- (62) Jin, S.; Du, W.; Wang, S.; Kang, X.; Chen, M.; Hu, D.; Chen, S.; Zou, X.; Sun, G.; Zhu, M. Thiol-Induced Synthesis of Phosphine-Protected Gold Nanoclusters with Atomic Precision and Controlling the Structure by Ligand/Metal Engineering. *Inorg. Chem.* **2017**, *S6*, 11151–11159.
- (63) Yuan, Y.; Cheng, L.; Yang, J. Electronic Stability of Phosphine-Protected Au₂₀ Nanocluster: Superatomic Bonding. *J. Phys. Chem. C* **2013**, *117*, 13276–13282.
- (64) Heaven, M. W.; Dass, A.; White, P. S.; Holt, K. M.; Murray, R. W. Crystal Structure of the Gold Nanoparticle $[N(C_8H_{17})_4]$ - $[Au_{25}(SCH_2CH_2Ph)_{18}]$. J. Am. Chem. Soc. **2008**, 130, 3754–3755.
- (65) Zhu, M.; Aikens, C. M.; Hollander, F. J.; Schatz, G. C.; Jin, R. Correlating the Crystal Structure of A Thiol-Protected Au₂₅ Cluster and Optical Properties. *J. Am. Chem. Soc.* **2008**, *130*, 5883–5885.
- (66) Haruta, M. Size- and Support-Dependency in the Catalysis of Gold. Catal. *Catal. Today* **1997**, *36*, 153–166.
- (67) Hashmi, A. S. K.; Hutchings, G. J. Gold Catalysis. *Angew. Chem., Int. Ed.* **2006**, 45, 7896–7936.
- (68) Chen, X. M.; Ma, N. N.; Zhang, Q. F.; Wang, J.; Feng, X. G.; Wei, C. G.; Wang, L. S.; Zhang, J.; Chen, X. N. Elucidation of the Formation Mechanism of Octahydrotriborate Anion (B₃H₈⁻) through the Nucleophilicity of the B–H Bond. *J. Am. Chem. Soc.* **2018**, *140*, 6718–6726.
- (69) Konishi, K.; Sugiuchi, M.; Shichibu, Y. Inherently Chiral Au₂₄ Framework with Double-Helical Hexagold Strands. *Angew. Chem., Int. Ed.* **2018**, *57*, 7855.